Electrically Conductive Sensors for Liquids Based on Quaternary Ethylene Vinyl Acetate (EVA)/Copolyamide/ Maleated-EVA/Polyaniline Blends

H. Cooper, E. Segal, S. Srebnik, R. Tchoudakov, M. Narkis, A. Siegmann

Department of Chemical Engineering and Department of Materials Engineering, Technion, IIT, Haifa 32000, Israel

Received 7 March 2005; accepted 27 March 2005
DOI 10.1002/app.21969
Published online in Wiley InterScience (www.interscience.wiley.com).

ABSTRACT: Electrically conductive blends, containing two immiscible polymers (ethylene vinyl acetate copolymer, EVA-19, and copolyamide 6/6.9, CoPA), polyaniline (PANI), and maleated EVA compatibilizer were studied as sensing materials for a homologous series of alcohols (methanol, ethanol, and 1-propanol). Recent results have shown that the corresponding uncompatiblized blends exhibited a preferred localization of PANI in the CoPA phase, leading to a cocontinuous morphology (i.e., both the CoPA phase and the PANI component located in it are continuous). The concept of the compatibilizer addition was to improve compatibility between the EVA-19 and the CoPA, modifying the morphology of the PANI-containing blend and altering its sensing properties. Extruded EVA-19/CoPA/maleated-EVA/PANI filaments produced by a capillary rheometer process at various shear rate levels were used for the sensing experiments. The filaments displayed high sensitivity levels upon exposure to the various alcohols as well as improved sensing stability and reproducibility at low compatibilizer contents. The sensing properties vary with compatibilizer concentration and are of inferior quality beyond a certain content. The sensing behavior of the compatibilized filaments is compared to the previously reported results for the corresponding uncompatibilized filaments. © 2006 Wiley Periodicals, Inc. J Appl Polym Sci 101: 110–117, 2006

Key words: sensors; plastics; blends; conductivity

INTRODUCTION

The increasing concern of environmental pollution and health or fire hazards due to various chemicals used in industry, together with the widespread requirements for more accurate process control, has created a need for new or improved sensing elements for measuring both physical and chemical parameters.[1,2] Intrinsically conductive polymers (ICPs) have been suggested as an effective medium for chemical sensing of airborne volatile compounds. Such conductive polymers offer chemical sensing ability due to electronic (conductivity) changes, arising with adsorption of the volatile compounds (analytes), and which are commonly attributed to the interaction of the electronically active analytes with either the polymer backbone itself or the dopant molecules incorporated within the polymer, thereby modulating the mobility and/or the number of available free charge carriers.[3]

There are numerous studies on ICP/polymer blends reported in the literature. These studies concluded that the ICP/polymer blends combine the advantageous mechanical properties of the host polymer with the electrical properties of the ICP. Thus, in the past few years, special attention has been focused on the application of ICP/polymer composites or blends as sensing materials. The responses of the blends are better defined compared with the neat conducting polymer.[2,4–8]

Recently, the sensing behavior of melt-processed polyaniline (PANI) containing immiscible polymer blends of ethylene vinyl acetate copolymer (EVA)/copolyamide 6/6.9 (CoPA) has been studied.[9] These blends were designed to have a double-percolation structure. The PANI phase showed a preferred localization within the minor-continuous CoPA phase, thus enhancing the formation of continuous conducting networks. A series of electrically conductive blends' filaments was produced by a capillary rheometer process. Liquid immersion/drying cycling of the filaments showed relatively high sensitivity and selectivity toward the studied liquids; however, the filaments' rate of production significantly affects the relative resistance change and their reproducibility. An attempt to improve the sensing properties of these filaments can be done by

Correspondence to: M. Narkis (narkis@tx.technion.ac.il).
Contract grant sponsor: U.S.–Israel Binational Science Foundation.
Contract grant sponsor: Levi Eshkol Scholarship from the Israel Ministry of Science.

the addition of EVA grafted with maleic anhydride (EVA-*g*-MA) compatibilizer.

This paper addresses the structure, electrical conductivity, and sensing properties of quaternary EVA-19/CoPA/maleated-EVA/polyaniline blends. The quaternary blends were used to produce a series of electrically conductive filaments by a capillary rheometer process at various shear rates. The filaments displayed high sensitivity levels upon exposure to various alcohols as well as improved sensing stability and reproducibility in comparison to the uncompatibilized blend.[9] The sensing properties varied with the compatibilizer content.

EXPERIMENTAL

Materials

The following materials were used:
Polyaniline. Versicon, polyaniline doped with *p*-toluene sulfonic acid (PANI-*p*TSA), conductivity = 6 S/cm; Zipperling Kessler, Germany;
Matrix polymer. Ethylene vinyl acetate copolymer (EVA-19), Greenflex ML50 (MFI = 2.5 g/10 min, VA content = 19%), Polimeri Europa, Italy;
Dispersed polymer. Copolyamide 6/6.9 (CoPA), a random copolymer, 51% [HN–$(CH_2)_5$–CO] and 49% [HN–$(CH_2)_6$–NH–CO–$(CH_2)_7$–CO], EMS, Switzerland;
Compatibilizer. EVA grafted with maleic anhydride (EVA-*g*-MA), containing less than 2 wt % MA, Overac, Atofina, France.

Blends preparation

Polymer pellets were ground to ensure good mixing. Dry-blended ternary mixtures containing [70 EVA-19/30 CoPA]/30 phr PANI with 2 or 5 phr compatibilizer (EVA-*g*-MA) were melt-mixed in a Brabender Plastograph, equipped with a 50 cm^3 cell, at 160 °C and 50 rpm for 12 min. The resulting blends were subsequently compression molded at 160 °C to obtain 3-mm-thick plaques.

Filaments preparation

Samples prepared by melt-mixing in the Brabender Plastograph were extruded into filaments using an Instron capillary rheometer mounted on an Instron TT-D machine, equipped with a capillary 5 cm (2 in.) long and 0.127 cm (0.05 in.) in diameter (L/D = 40) at extrusion temperature of 160 °C. The blends were extruded at various crosshead speeds, ranging from 0.05 to 50 cm/min, providing an approximate shear rate range of 3–3000 s^{-1}. The filaments were collected and used for electrical conductivity measurements, sensor experiments, and morphology characterization.

Electrical conductivity measurements

The electrical conductivity of compression-molded specimens was measured (DIN-53,596) using a Keithley Electrometer 175A instrument and a 240A high-voltage supply from Keithley Instruments. For samples of high conductivity levels a Keithley Electrometer 6514, a Keithley Electrometer 175A, and an Elscint power supply model TTPS-3 were used.

For measuring a filament's conductivity, silver paint was applied on the filaments' surface at several locations (regularly spaced) to ensure contact between the sample and the electrodes and thus to minimize the contact resistance. The longitudinal resistance between two silver marks was measured (by the Keithley Electrometer 175A), and the electrical conductivity was calculated. Resistance was measured at several locations of each filament and averaged to ensure reliable results. Conductivities below 10^{-8} S/cm were beyond the limit of the measuring device.

Sensor analysis

For sensor analysis, 5-mm-long filaments were used. A small amount of silver paint was applied at the filaments' ends where electric wires were connected (the silver paint's resistivity was insensitive to the studied solvents). Liquid sensing experiments were performed by immersing/drying cycles at ~25 °C along with continuous monitoring of the changing resistance. A detailed description of the electrical measurement apparatus is given elsewhere.[10,11]

All data are presented as relative resistance, i.e., R_t/R_0, where R_0 is the initial resistance of the sensor and R_t is the measured resistance at time t. The solvents used in this study include methanol, ethanol, and 1-propanol.

Morphological characterization

Scanning electron microscopy (SEM) of freeze-fractured surfaces was performed using a Jeol JSM 5400 at an accelerating voltage of 10 kV. Samples were gold-sputtered prior to observation.

RESULTS AND DISCUSSION

Compression molded samples

The effect of EVA-*g*-MA compatibilizer on the morphology of the 70 EVA-19/30 CoPA blend is depicted in Figure 1. The addition of 2 phr EVA-*g*-MA (Fig. 1a) does not result in a significant observable effect. The adhesion level between the dispersed CoPA particles and the EVA matrix is relatively weak, as depicted by the gaps between the two polymers. This weak adhesion is further manifested by some CoPA particles, detached from the matrix, as depicted by the spherical

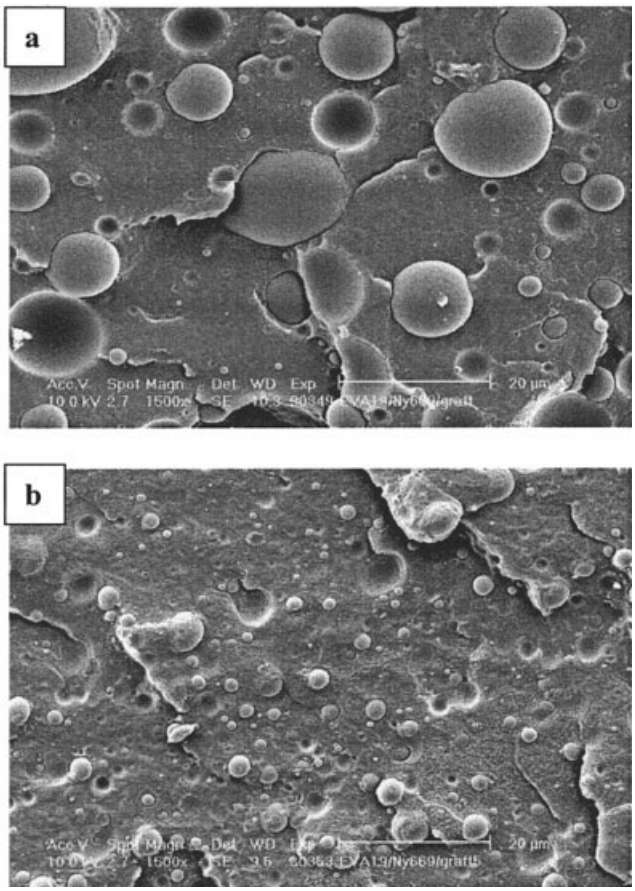

Figure 1 SEM micrographs of freeze-fracture surfaces of compression molded 70 EVA-19/30 CoPA blends containing (a) 2 phr EVA-*g*-MA and (b) 5 phr EVA-*g*-MA.

cavities in Figure 1a. The size of the dispersed CoPA particles is ~7 μm, similar to the uncompatibilized blend shown elsewhere,[9] and their size distribution is rather broad. However, the addition of 5 phr EVA-*g*-MA [Fig. 1(b)] results in a significant reduction of the CoPA particle size (to ~4 μm). Furthermore, in some regions, the boundaries between the dispersed phase and the matrix are hardly distinguished, indicating an improved interfacial adhesion level. These result from the decreased dispersed phase level of coalescence, through stabilization of the interface and reduction of the interfacial tension by the compatibilizer.[12,13]

Extruded filaments

Resistivity–shear rate relations

A capillary rheometer process was used to produce extruded filaments at varying shear rate levels, and their resistivity was measured. Figure 2 shows the effect of extrusion shear rate on the resistivity dependence of [70 EVA-19/30 CoPA]/30 phr PANI blends, containing 0, 2, and 5 phr EVA-*g*-MA. The compression-molded specimens exhibited resistivities of 5.4 $\times$ 10^3, 2.5 $\times$ 10^3, and 4.4 $\times$ 10^3 Ω-cm for the 0, 2, and 5 phr EVA-*g*-MA compositions, respectively.

Extruded filaments containing 0 and 2 phr EVA-*g*-MA (Fig. 2) maintain relatively low resistivity values of approximately 10^3–10^4 Ω-cm throughout the studied extrusion shear rate range. The blend containing 5 phr EVA-*g*-MA exhibits a complex and interesting resistivity–extrusion shear rate relationship, where at low and intermediate shear rate levels the resistivity of the filaments is high (>10^8 Ω-cm). However, at shear rate levels higher than 100 s^{-1}, a dramatic resistivity decrease is observed and the filaments maintain a resistivity level of ~10^5 Ω-cm through the high shear rate range.

The morphology of uncompatibilized [70 EVA-19/30 CoPA]/PANI blends was previously reported[9] and showed a preferred localization of PANI within the CoPA phase. This effect leads to a co-*co*-continuous morphology, where both the CoPA phase and the PANI component located in it are continuous, thus enhancing the formation of continuous conducting networks through the formation of a double-percolating structure (CoPA and PANI).

Figure 3 depicts the surface morphology of filaments containing 2 and 5 phr EVA-*g*-MA, extruded at an intermediate shear rate level (60 s^{-1}), and of filaments containing 5 phr EVA-*g*-MA, extruded at a high shear rate level (600 s^{-1}). The 5 phr EVA-*g*-MA filaments, extruded at 60 s^{-1} [Fig. 3(a)], depict extremely

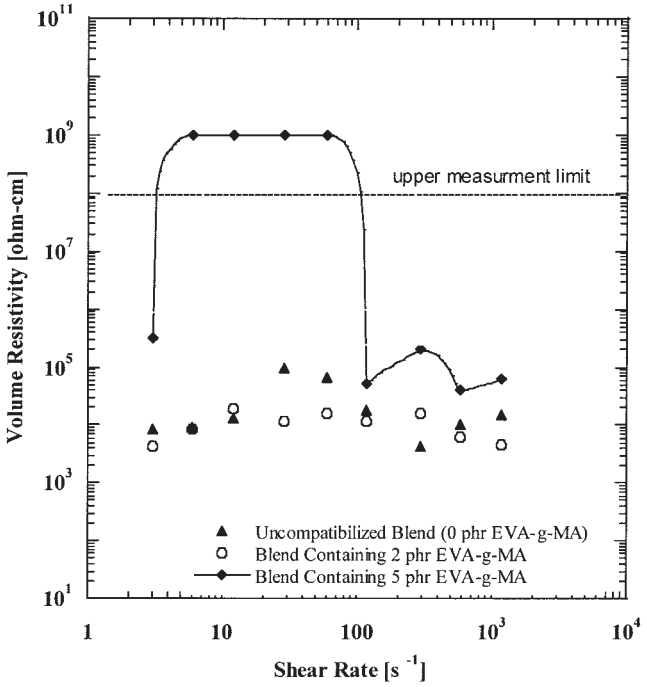

Figure 2 Resistivities versus extrusion shear rate of [70 EVA-19/30 CoPA]/30 phr PANI filaments containing 0, 2, and 5 phr EVA-*g*-MA.

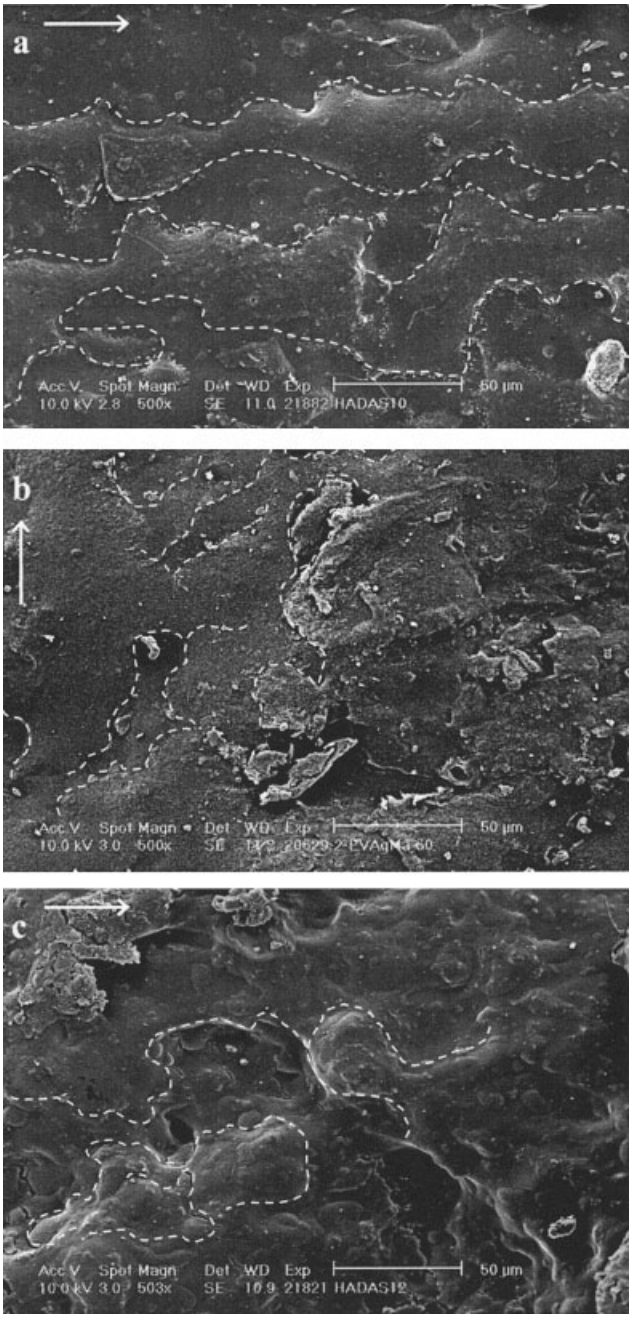

Figure 3 SEM micrographs of external surfaces of [70 EVA-19/30 CoPA]/30 phr PANI filaments: (a) 5 phr EVA-*g*-MA, (b) 2 phr EVA-*g*-MA, both extruded at 60 s^{-1}, and (c) 5 phr EVA-*g*-MA, extruded at 600 s^{-1}. The arrow represents the flow direction.

large isolated elongated regions of the CoPA phase (outlined). The 2 phr EVA-*g*-MA filaments, extruded at 60 s^{-1} [Fig. 3(b)], and the 5 phr EVA-g-MA filaments, extruded at 600 s^{-1} [Fig. 3(c)], exhibit, however, a finer dispersion of the CoPA phase (outlined) within EVA-19. Etching of the CoPA by immersing the filaments in methanol (for 20 min) exposes the PANI particles (preferentially located within the CoPA phase). Large PANI particles, some of them embedded in the remnants of the CoPA phase, are observed for the 5 phr EVA-*g*-MA filaments, extruded at 60 s^{-1} [Fig. 4(a)]. The size of the PANI-containing CoPA clusters is more than 50 μm. These clusters' size is reduced in the 2 phr EVA-*g*-MA filaments, extruded at 60 s^{-1} [Fig. 4(b)]. In the 5 phr EVA-*g*-MA filaments, extruded at 600 s^{-1} [Fig. 4(c)], the PANI particles appear to be dispersed in smaller CoPA clusters throughout the entire blend. Figures 3 and 4 demonstrate that the dispersion level of CoPA within EVA-19

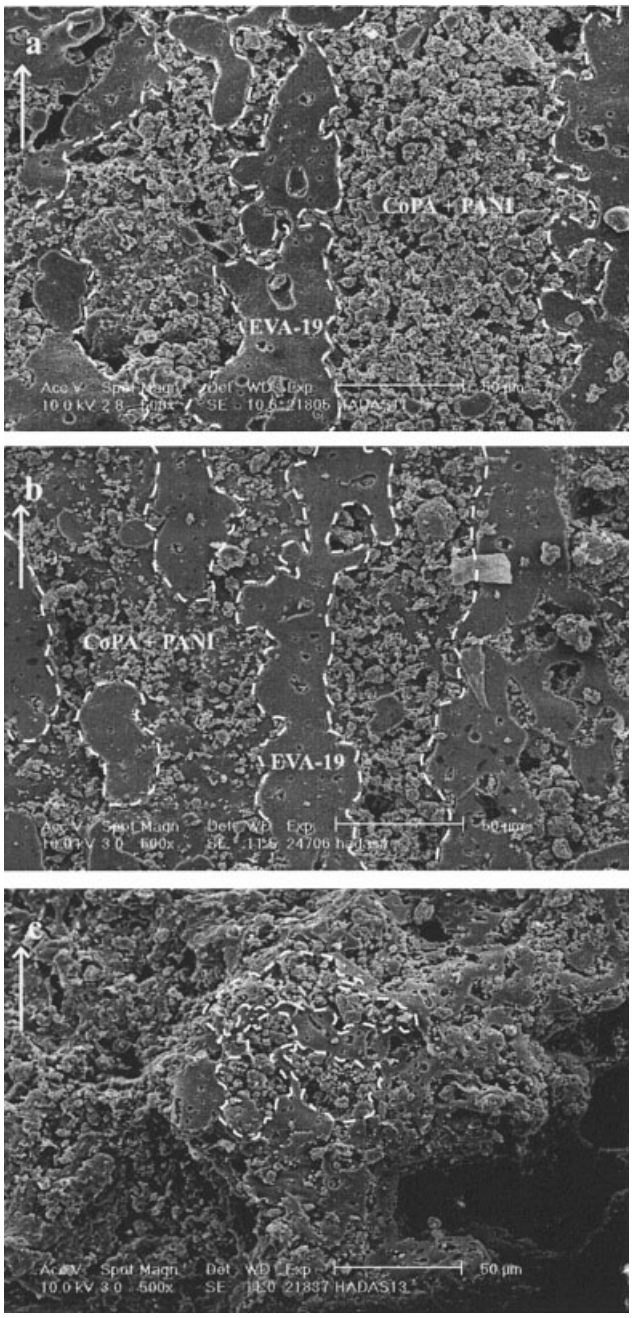

Figure 4 SEM micrographs of methanol etched external surfaces of [70 EVA-19/30 CoPA]/30 phr PANI filaments containing: (a) 5 phr EVA-*g*-MA, (b) 2 phr EVA-*g*-MA, both extruded at 60 s^{-1}, and (c) 5 phr EVA-*g*-MA extruded at 600 s^{-1}.

is finer in the 2 phr EVA-*g*-MA filaments, extruded at 60 s^{-1}, and the 5 phr EVA-*g*-MA filaments, extruded at 600 s^{-1}.

It seems that the excess EVA-*g*-MA, located at the CoPA/PANI interface, improves the adhesion between the two polymers (EVA and CoPA) but does not help in the dispersion of the PANI particles. At the higher shear rate level fracturing of the CoPA phase is enhanced resulting in improved levels of its dispersion. The effect of both lower shear rate and higher compatibilizer content on the structure is clearly exhibited by the resistivity–shear rate data; the large CoPA regions combined with poor dispersion of PANI result in insulating filaments.

The results in Figures 3 and 4 can be partly understood from a theoretical standpoint. The addition of a compatibilizer suppresses coalescence in both quiescent and flow conditions, although the exact mechanism of the latter case is not fully understood. In quiescent conditions, average drop size of the minority phase decreases monotonically with compatibilizer concentration up to a critical value, which corresponds to the limiting concentration of compatibilizer located at the interface between the two immiscible polymer phases. Flow conditions present a more complicated picture. In general, shearing slows down coarsening in polymer blends, leading to metastable drop size that is dependent on shear rate.[14] However, there are at least two opposing forces that determine the compatibilized polymer morphology.[15] The Marangoni force (the tangential stress due to surface concentration gradients of the compatibilizer) acts to suppress deformation of the drops and their coalescence in a similar manner to that of increased viscosity of the dispersed phase, by reducing the mobility of the interface.[16] On the other hand, the decrease in interfacial tension promotes deformation of the drops. These two opposing effects lead to a stabilized structure of a finite size in the flow direction. However, since the effect of a compatibilizer on drop deformation decreases with increasing shear rate,[17] the difference in the observed morphologies between the two concentrations (Fig. 3) at 60 s^{-1} is not as visible as that observed under quiescent conditions (Fig. 1). The good dispersion of the CoPA phase observed at high shear rates is a kinetically frozen morphology that is due to breaking up of large CoPA regions into smaller ones, on the one hand, and prevention of coalescence on the other hand.[14,17]

Viscosity–shear rate relations

The apparent viscosity of the [70 EVA-19/30 CoPA]/30 phr PANI blends containing 0, 2, and 5 phr EVA-*g*-MA was studied using the capillary rheometer at 160 °C and is depicted in Figure 5. A similar behavior of PANI-containing systems was observed by Segal et al.,[18] who investigated the behavior of polystyrene (PS)/PANI blends prepared by an aqueous-dispersion blending method. Rheological studies have shown that the neat PS matrix exhibited higher viscosity values than the PS/PANI blend, while an opposite trend was expected. This behavior was related to slip-at-the-wall effects caused by the PANI presence within the PS matrix. Since the PANI content in the blends shown in Figure 5 is relatively high, the presence of slip effects was investigated; neat 70 EVA-19/30 CoPA blend and the blend containing 30 phr PANI were compared. There was a significant difference in the viscosity values of the PANI containing blend as measured by two different capillaries, while similar values were obtained for the reference blend. Hence, there were slip-at-the-wall effects due to the PANI presence also within the EVA19/CoPA matrix. The viscosity versus shear rate behavior (Fig. 5) shows that throughout the entire range of shear rates both the 2 and 5 phr EVA-*g*-MA blends exhibit similar viscosity values, but values lower than that of the uncompatibilized one.

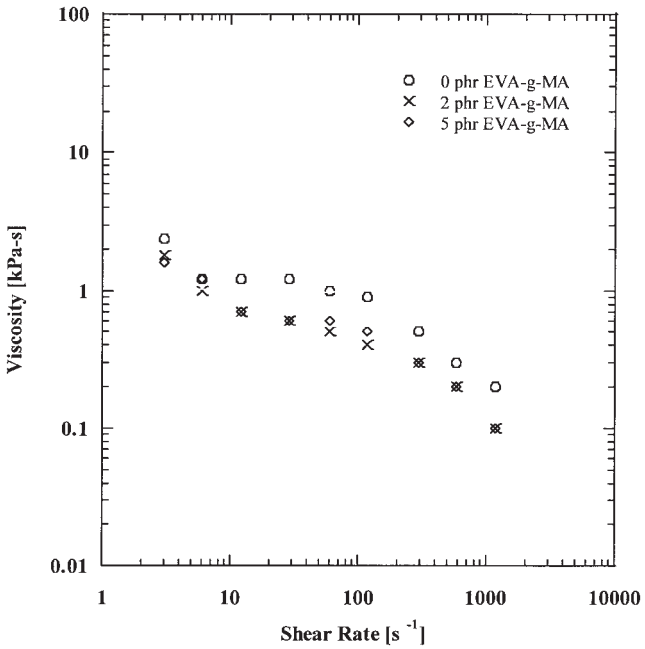

Figure 5 Apparent viscosity versus shear rate of [70 EVA-19/30 CoPA]/30 phr PANI blends containing 0, 2, and 5 phr EVA-*g*-MA.

The effect of compatibilizers on the rheological properties of polymers has been previously discussed.[19–21] Both an increasing and a decreasing viscosity was reported, especially at lower shear rates.

Sanchez-Solis[21] have reported a similar behavior to that found currently, whereupon the viscosity decreases with the addition of a compatibilizer. The reduction in viscosity values upon addition of a compatibilizer was observed by comparison of polyethylene terephthalate (PET)/styrene butadiene rubber

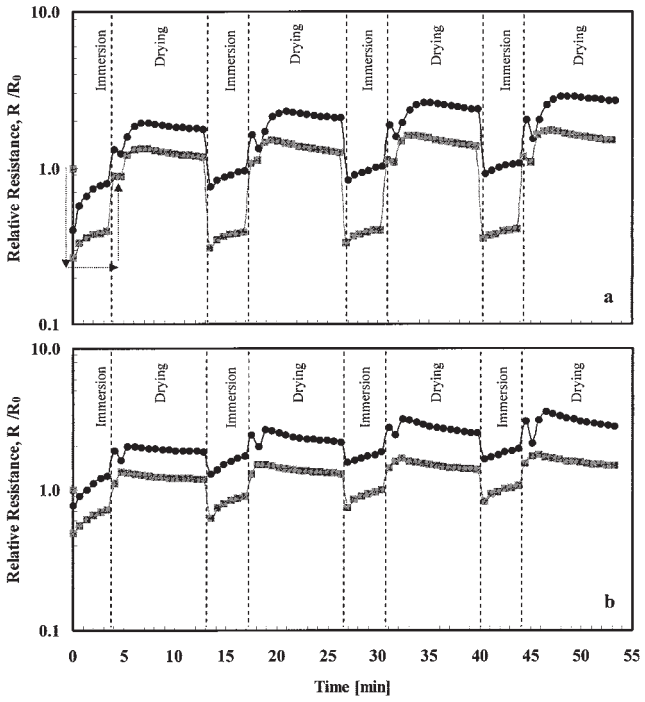

Figure 6 Relative resistance versus exposure time to different alcohols: (a) methanol, (b) ethanol, and (c) 1-propanol) of (●) [70 EVA-19/30 CoPA]/30 phr PANI filaments, and (■) [70 EVA-19/30 CoPA]/30 phr PANI/2 phr EVA-*g*-MA filaments, extruded at 600 s^{-1}. The arrows represent the relative resistance change of the first immersion cycle.

(SBR) physical blends with blends containing PET and MA-functionalized SBR (SBRg). The viscosity decreased with an increasing SBRg content up to 30 phr. It was suggested that the inhibition of coalescence, caused by the compatibilizer, combined with the breakage of agglomerates by the high shear stresses lead to an overall viscosity decrease. This mechanism may explain the viscosity decrease observed in the present studied blends (Fig. 5); it is also supported by the blends' morphology [Fig. 1(b)], where the addition of 5 phr EVA-*g*-MA to the 70 EVA-19/30 CoPA blend results in a significant reduction of the CoPA particle size.

Sensing properties

The compatibilized filaments were exposed to a homologous series of alcohols (methanol, ethanol, and 1-propanol) and their resistance was monitored. In each cycle, filaments were immersed for 3 min in a given alcohol and then allowed to dry in air for 7 min. Four sequential cycles were performed for each specimen. Each data point in Figures 6 and 7 represents an average of three different filaments. The sensing properties of the compatibilized PANI blends were compared with the corresponding uncompatibilized blends.[9]

Filaments containing 2 phr EVA-*g*-MA

At all shear rates (not shown), the compatibilized filaments have shown the highest sensitivity to methanol. A similar behavior was previously observed for neat PANI films[22,23] and for the uncompatibilized blend.[9] The higher affinity of the methanol molecules to the PANI particles, compared to ethanol and 1-propanol, was identified as the dominant effect and was discussed elsewhere.[9] The compatibilized filaments produced at 6 and 60 s^{-1} (not shown) did not depict significant differences in the sensing behavior compared to the corresponding uncompatibilized filaments. However, the sensitivity of the 600 s^{-1} compatibilized filaments toward the three examined alcohols was improved compared to the uncompatibilized filaments.

The relative resistance variations (R_t/R_0) of the uncompatibilized and compatibilized (2 phr EVA-*g*-MA)

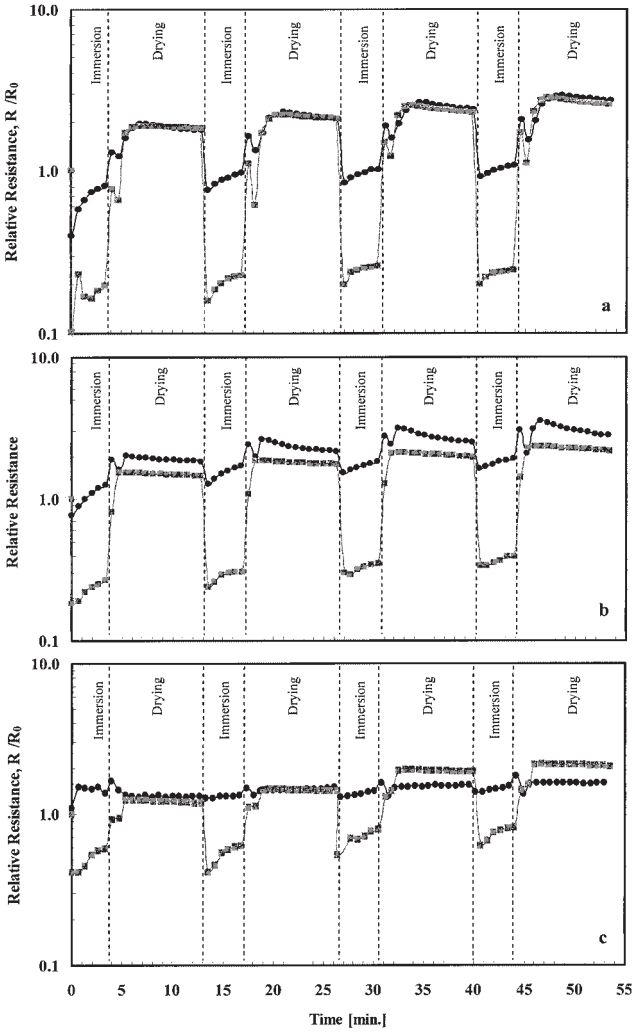

Figure 7 Relative resistance versus exposure time to different alcohols: (a) methanol, (b) ethanol, and (c) 1-propanol of (● [70 EVA-19/30 CoPA]/30 phr PANI filaments and ■ [70 EVA-19/30 CoPA]/30 phr PANI/5 phr EVA-*g*-MA filaments, extruded at 600 s^{-1}.

filaments extruded at a shear rate of 600 s^{-1} are shown in Figure 6. All the filaments display a decreasing resistance upon exposure to the various alcohols; however, the compatibilized filaments show an improved sensitivity (higher resistance decrease or lower relative resistance value) compared with the uncompatibilized filaments (e.g., relative resistance of 0.27 versus 0.40 upon exposure to methanol, 0.49 versus 0.77 upon exposure to ethanol). Upon exposure to methanol [Fig. 6(a)], the resistance of the compatibilized filaments is almost constant during the immersion cycle (i.e., good resistance stability) and tends to return to its initial value upon drying. The resistance values obtained in the drying cycles of the compatibilized filaments exposed to methanol and ethanol are relatively close to the initial resistance value. Upon exposure to 1-propanol [Fig. 6(c)], the resistivity change of the compatibilized filaments is quite pronounced.

Filaments containing 5 phr EVA-*g*-MA

The sensing behavior of the compatibilized filaments, containing 5 phr EVA-*g*-MA, was also compared to the sensing behavior of the corresponding uncompatibilized filaments. Remarkable differences are again observed for filaments extruded at a high shear rate level of 600 s^{-1}. The compatibilized filaments (Fig. 7) show a significantly higher sensitivity to all studied alcohols compared to the uncompatibilized filaments (e.g., relative resistance of 0.10 versus 0.40 upon exposure to methanol, 0.18 versus 0.77 upon exposure to ethanol) and to the filaments containing 2 phr EVA-*g*-MA (Fig. 6). Upon drying, the resistance values of the compatibilized filaments exposed to methanol [Fig. 7(a)] are much higher than the initial values. However, upon exposure to ethanol [Fig. 7(b)], the resistance values obtained in the drying cycles of the compatibilized filaments are closer to the initial resistance. For the compatibilized filaments exposed to 1-propanol [Fig. 7(c)], the sensing behavior shows again high resolution. Despite the higher sensitivity of the 5 phr EVA-*g*-MA filaments compared to the 2 phr EVA-*g*-MA filaments, their resistance values in the drying cycles are much higher than the initial values and their resistance reproducibility within the proceeding cycles is of inferior quality compared with the 2 phr EVA-*g*-MA filaments. The reason for this behavior is not clear, but it implies that there is an optimal compatibilizer content.

Uncompatibilized versus compatibilized filaments

When comparing the sensing behavior of the uncompatibilized filaments to the compatibilized filaments (Figs. 6 and 7), except for the significant difference in the sensitivity, other differences are observed. Usually higher resistance values are obtained in the drying cycles of the uncompatibilized filaments exposed to methanol and ethanol, meaning that their reversibility is of inferior quality. Upon exposure to 1-propanol, the uncompatibilized filaments show almost constant resistance values throughout the four consecutive cycles, with no observable resolution. The irreversibility phenomenon during drying ($R_t/R_0 > 1$) of the uncompatibilized filaments (extruded at 600 s^{-1} and exposed to methanol) was previously discussed and related to permanent changes in the filaments' morphology.[9] Large cavities were formed as a result of the detachment of CoPA and PANI particles. It was suggested that some PANI particles were removed during immersion, disrupting the PANI network continuity, resulting in an irreversible sensor behavior.

The resistance reduction of PANI systems upon exposure to high polar liquids (such as methanol) has been previously reported.[24–28] Different mechanisms were proposed to explain the enhanced conductivity. Usually, with neat PANI systems, it is a result of variations in the intrinsic electrical conductivity of the doped PANI. Another possible mechanism is based on the model of "metallic islands." Accordingly, the doping process of PANI is nonhomogeneous, involving the formation of small, completely doped three-dimensional islands of the polymer in a matrix of the nondoped fraction. As doping further proceeds, the islands increase in size and new islands are formed. These islands are surrounded by insulating "beaches" through which charge energy limited tunneling occurs, permitting conduction from one island to another. It was suggested that water molecules facilitate the conduction through these beaches, probably by reducing the effective height or width of the tunneling barrier.[28] Thus, with increasing water content, the apparent separation of the conductive islands and/or the height of the barrier between the conductive islands decrease, making tunneling more favorable. The foregoing explanation can be expanded to polymer/PANI blends, where the conductive PANI clusters/domains are dispersed in an insulating matrix. It was suggested that the absorbed polar liquid molecules interact with the PANI moieties and transfer electronic charge,[2] increasing conductivity. Accordingly, the sorbed analyte molecules in the EVA-19/CoPA/PANI blends interact with the PANI particles; the electrical conductivity is mainly controlled by hopping/tunneling processes of charge carriers between these conducting PANI clusters.

The higher sensitivity, improved sensing stability, and reproducibility of the compatibilized filaments, extruded at 600 s^{-1} (Figs. 6 and 7), suggest that the compatiblizer plays an important role in the high shear rate filaments (at the lower shear rates no significant differences in the sensing behavior, compared to the corresponding uncompatibilized filaments,

were observed). The addition of EVA-*g*-MA results in an improved interfacial adhesion level between CoPA and EVA-19 as well as in an improved dispersion mode of the CoPA phase within the EVA-19 matrix (Figs. 3 and 4). These changes improve the sensing properties of the compatibilized filaments compared to the uncompatibilized filaments. It should be emphasized that the compatibilized filaments show a similar morphology (not shown), despite being better sensors. In the latter, the removal of PANI particles was probably not as significant as in the uncompatibilized filaments.

In summary, this article demonstrates that compatibilized EVA-19/CoPA/PANI blends are significantly more sensitive and thus more selective to the examined liquids compared with the corresponding uncompatibilized blends. As higher compatibilizer content is applied, the sensitivity is enhanced; however, other sensing properties, such as reproducibility, decrease in their quality. Thus, whereas blends containing relatively low compatibilizer content exhibit lower sensitivity for the examined polar liquids, blends containing higher compatibilizer content may lack resistivity reproducibility.

CONCLUSIONS

Compatibilized EVA-19/CoPA/PANI blends exhibit a double-continuity phase structure. The majority of the compatibilizer (EVA-*g*-MA) is assumed to be located at the EVA-19/CoPA interface, resulting in a significant reduction of the CoPA particles size and an improved interfacial adhesion level.

The combination of both shear rate level and compatibilizer content affects the resistivity behavior of compatibilized EVA-19/CoPA/PANI blends. At relatively low shear rate levels and relatively high compatibilizer contents, the fracturing of the CoPA phase is limited and thus causes poor dispersion of PANI resulting in high resistivity values.

The PANI containing 70EVA-19/30CoPA blends show capillary rheological measurements affected by slip-at-the-wall. The compatibilized blends show lower viscosity values compared with the corresponding uncompatibilized filaments, mainly due to breakage of agglomerates by the higher shear stresses and inhibition of coalescence.

Compatibilized EVA-19/CoPA/PANI filaments, produced at high shear rate levels, exhibit higher sensitivity, improved sensing stability, and reproducibility compared with the corresponding uncompatibilized filaments. This behavior is due to the enhanced dispersion level of the CoPA clusters and the improved EVA-19/CoPA interfacial adhesion. Significant improved sensing stability and reproducibility were displayed upon the addition of relatively low compatibilizer contents. With higher compatibilizer contents, enhanced sensitivity levels are obtained; however, the resistance reproducibility decreases.

References

1. Miasik, J. J.; Hooper, A.; Tofield, B. C. J Chem Soc Faraday Trans 1 Phys Chem Cond Phases 1986, 82, 117.
2. Unde, S.; Ganu, J.; Radhakrishnan, S. Adv Mater Optics Electron 1996, 6, 151.
3. Collins, G. E., Buckley, L. J. Synth Met 1996, 78, 93.
4. Koul, S.; Dhawan, S. K.; Chandra, R. SPIE 1999, 3903, 278.
5. Koul, S.; Chandra, R.; Dhawan, S. K. Sensors Actuators B Chem 2001, 75, 151.
6. Matsuguchi, M.; Io, J.; Sugiyama, G.; Sakai, Y. Synth Met 2002, 128, 15.
7. Matsuguchi, M.; Okamoto, A.; Sakai, Y. Sensors Actuators B Chem 2003, 94, 46.
8. Lin, C. W.; Hwang, B. J.; Lee, C. R. J Appl Polym Sci 1999, 73, 2079.
9. Cooper, H.; Segal, E.; Srebnik, S.; Tchoudakov, R.; Narkis, M.; Siegmann, A. Polym Adv Tech 2004, 15, 573.
10. Segal, E.; Tchoudakov, R.; Narkis, M.; Siegmann, A. Polym Eng Sci 2002, 42, 2430.
11. Segal, E.; Tchoudakov, R.; Narkis, M.; Siegmann, A. J Polym Sci B Polym Phys 2003, 41, 1428.
12. Moly, K. A.; Oommen, Z.; Bhagawan, S. S.; Groeninckx, G.,; Thomas, S. J Appl Polym Sci 2002, 86, 3210.
13. Sundarraj, U.; Macosko, C. W. Macromolecules 1995, 28, 2647.
14. Zvelindovsky, A. V.; Sevink, G. J. A.; Lyakhova, K. S.; Altevogt, P. Macromol Theory Simul 2004, 13, 140.
15. Fortelny, I. Eur Polym Mater 2004, 40, 2161.
16. Pawar, Y.; Stebe, K. J Phys Fluids 1996, 8, 1738.
17. Van Puyvelde, P.; Velankar, S.; Moldenaers, P. Curr Opin Colloid Interface Sci 2001, 6, 457.
18. Segal, E.; Haba, Y.; Narkis, M.; Siegmann, A. J Polym Sci B Polym. Phys 2001, 39, 611.
19. Kon Kim, J.; Lee, H. Polymer 1996, 37, 305.
20. Marco, C.; Ellis, G.; Gomez, M. A.; Fatou, J. G.; Arribas, J. M.; Campoy, I.; Fontecha, A. J Appl Polym Sci 1997, 65, 2665.
21. Sanchez-Solis, A.; Calderas, F.; Manero, O. Polymer 2001, 42, 7335.
22. Boyle, A.; Genies, E. M.; Lapkowski, M. Synth Met 1989, 28, C769.
23. Athawale, A. A.; Kulkarni, M. V. Sensors Actuators B Chem 2000, 67, 173.
24. Tan, C. K.; Blackwood, D. J. Sensors Actuators B 2000, 71, 184.
25. Matveeva, E. S. Synth Met 1996, 79, 127.
26. Nechtschein, M.; Santier, C.; Travers, J. P.; Chroboczek, J.; Alix, A.; Ripert, M. Synth Met 1987, 18, 311.
27. Travers, J. P.; Nechtschein, M. Synth Met 1987, 21, 135.
28. Javadi, H. H. S.; Zuo, F.; Angelopoulos, M.; MacDiarmid, A. G. Mol Cryst Liquid Cryst 1988, 160, 225.